# Local and Long-Range Interactions in the Thermal Unfolding Transition of Bovine Pancreatic Ribonuclease A†

Amiel Navon,‡ Varda Ittah,‡ John H. Laity,§ Harold A. Scheraga,*,§ Elisha Haas,*,‡ and Eugene E. Gussakovsky‡

*Faculty of Life Sciences, Bar Ilan University, Ramat Gan 52900, Israel, and Baker Laboratory of Chemistry and Chemical Biology, Cornell University, Ithaca, New York 14853-1301*

*Received August 16, 2000; Revised Manuscript Received October 25, 2000*

ABSTRACT: This research was undertaken to distinguish between local and global unfolding in the reversible thermal denaturation of bovine pancreatic ribonclease A (RNase A). Local unfolding was monitored by steady-state and time-resolved fluorescence of nine mutants in each of which a single tryptophan was substituted for a wild-type residue. Global unfolding was monitored by far-UV circular dichroism and UV absorbance. All the mutants (except F8W and D38W) exhibited high specific enzymatic activity, and their far-UV CD spectra were very close to that of wild-type RNase A, indicating that the tryptophan substitutions did not affect the structure of any of the mutants (excluding K1W and Y92W) under folding conditions at 20 °C. Like wild-type RNase A, the various mutants exhibited reversible cooperative thermal unfolding transitions at pH 5, with transition temperatures 2.5−11 °C lower than that of the wild-type transition, as detected by far-UV CD or UV absorbance. Even at 80 °C, well above the cooperative transition of all the RNase A mutants, a considerable amount of secondary and tertiary structure was maintained. These studies suggest the following two-stage mechanism for the thermal unfolding transition of RNase A as the temperature is increased. First, at temperatures lower than those of the main cooperative transition, long-range interactions within the major hydrophobic core are weakened, e.g., those involving residues Phe-8 (in the N-terminal helix) and Lys-104 and Tyr-115 (in the C-terminal $\beta$-hairpin motif). The structure of the chain-reversal loop (residues 91−95) relaxes in the same temperature range. Second, the subsequent higher-temperature cooperative unfolding transition is associated with a loss of secondary structure and additional changes in the tertiary contacts of the major hydrophobic core, e.g., those involving residues Tyr-73, Tyr-76, and Asp-38 on the other side of the molecule. The hydrophobic interactions of the C-terminal loop of the protein are enhanced by high temperature, and perhaps are responsible for the preservation of the local structural environment of Trp-124 at temperatures slightly above the major cooperative transition. The results shed new light on the thermal unfolding transitions, generally supporting the thermal unfolding hypothesis of Burgess and Scheraga, as modified by Matheson and Scheraga.

The cooperative thermal unfolding of ribonuclease A (RNase A)[1] with intact disulfide bonds has been shown to be a reversible two-state transition in neutral or mildly acidic solutions (*1*−*12*), but becomes irreversible as the pH increases above 7 (*2*). There are, however, indications of multiple steps in the thermal transition (*13*−*25*, *70*), for which a mechanism has been proposed (*15*, *18*, *70*) with subsequent varying degrees of supporting experimental evidence (*18*, *26*−*31*, *70*). It is, therefore, of interest to obtain further evidence to determine whether the unfolding process is really a single transition or consists of a series of local and global transitions. This question can be approached by using fluorescence-based spectroscopic measurements and site-directed mutagenesis to introduce fluorophores into various parts of the RNase A molecule. Since wild-type RNase A does not contain any tryptophans, this residue is ideal for such substitutions and, in fact, had already been used in studies in which Tyr-92 (*32*) and Phe-120 (*9*) were replaced with Trp.

The goal of this work was to investigate the local and global conformational changes that occur during the thermal unfolding transition of RNase A by a multiple-probe approach, using nine different mutants in which Trp was inserted as a single-site substitution for mainly surface residues in each mutant. The thermal unfolding of each mutant was monitored by UV CD spectroscopy, UV absorption, and tryptophan fluorescence. The nine residues replaced with tryptophan were scattered over the surface of the RNase A molecule, viz., Lys-1, Phe-8, Asp-38, Tyr-73, Tyr-76, Tyr-92, Lys-104, Tyr-115, and Val-124 (see Figure 1) (*33*). Local thermal unfolding transitions were found by Trp fluorescence in some of the mutants at temperatures lower than those of the corresponding global thermal unfolding transitions detected by far-UV CD or UV absorption.

† This research was supported by Grants GM-39372 and GM-24893 from the National Institutes of Health and by grants from the Israel Science Foundation and the U.S.-Israel Binational Science Foundation. This work was also supported by the National Foundation for Cancer Research.

‡ Bar Ilan University.

§ Cornell University.

[1] Abbreviations: RNase A, bovine pancreatic ribonuclease A; wt-RNase A, wild-type RNase A; $W^m$-RNase A, mutant RNase A with residue *m* replaced with tryptophan; HEPES, *N*-(2-hydroxyethyl)-piperazine-*N*′-2-ethanesulfonic acid; O-T-16, the 16th peptide from a chromatographic analysis of the tryptic hydrolysis of oxidized RNase A; HPLC, high-performance liquid chromatography; SDS−PAGE, polyacrylamide gel electrophoresis in sodium dodecyl sulfate; UV, ultraviolet; CD, circular dichroism; TF, tryptophan fluorescence.

10.1021/bi001945w CCC: $20.00 
Published on Web 12/09/2000

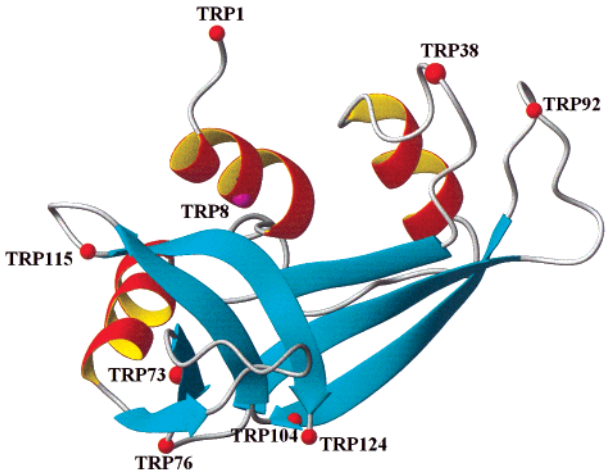


FIGURE 1: Ribbon diagram of bovine pancreatic ribonuclease A, taken from a high-resolution X-ray crystal structure (*33*) and showing the locations of the nine point mutations studied here. The added tryptophans sample most of the major structural elements of RNase A, including the major $\beta$-hairpin region (D38W and Y92W), the N-terminal helix region (K1W and F8W), and the major hydrophobic core region (Y73W, Y76W, K104W, Y115W, and V124W).

## MATERIALS AND METHODS

*Materials.* All enzyme preparations and other chemicals were purchased from Boehringer Mannheim or Sigma, unless stated otherwise. L-Tryptophan from Sigma was used without further purification.

*Production and Purification of Recombinant RNase A.* RNase A mutants were prepared by point mutagenesis and purified as described by del Cardayré et al. (*34*) and Laity et al. (*35*). The plasmids were sequenced at the Department of Biological Services of the Weizmann Institute (Rehovot, Israel). The final recombinant protein products were purified by ion-exchange chromatography (*35*), and their purity was checked by SDS−PAGE analysis. The enzymatic activities of all species were determined by the procedure described previously (*35*).

*Spectroscopic Measurements.* Four types of spectroscopic measurements were made: near- and far-UV circular dichroism (CD), UV absorption, and tryptophan fluorescence. All experiments were carried out in 5−20 mM sodium acetate buffer (pH 5.0). The near-UV CD, UV absorption, and fluorescence measurements were made by using a quartz cell with a path length of 1.00 cm, whereas the far-UV CD measurements employed a quartz cell with a path length of 0.020 cm.

Circular dichroism spectra were measured at various temperatures with a model 62A DS CD spectrometer (Aviv Associates, Lakewood, NJ) calibrated with a camphorsulfonic acid solution (*36*, *37*). Equilibrium far-UV CD spectra were obtained at 20 and 80 °C in 5−20 mM sodium acetate buffer (pH 5.0), while near-UV spectra were obtained only at 20 °C under the same conditions. The raw CD measurements (in millidegrees) were converted to molar ellipticity [Θ] and mean residue ellipticity $[\Theta]_m$ (in degrees × square centimeter per decimole) using molecular weight values computed from the amino acid composition (Table 1). The secondary structure content was calculated from the far-UV CD spectra in the 190−250 nm wavelength range by the procedure and computer program CONTIN developed by Provencher and Glöckner (*38*−*40*). The far-UV CD spectra of 17 proteins (*41*) obtained at 20 °C were used as a reference set for secondary structure analysis. Four spectra of denatured proteins (*42*) were added to the reference set used for analysis

Table 1: Parameters of Absorption, Far-UV CD Spectra, and Secondary Structure of Wild-Type RNase A and Its Tryptophan Derivatives at pH 5.0 and 20 °C (and at 20 °C after heating to 80 °C)[a]

| mutant | MW[b] | $\epsilon$[c] | [Θ][d] | $\lambda$[d] (nm) | $[\Theta]_m$[d] | $\lambda_m$[d] (nm) | α[e] (%) | $\beta$[e] (%) | turn[e] (%) | $r$[e] (%) |
|---|---|---|---|---|---|---|---|---|---|---|
| wild type | 13682 | 9.8 ± 0.2 | −30.8 ± 0.3 | 275 | −11.4 ± 0.3 | 208 | 22 ± 0.7 | 34 ± 1.3 | 24 ± 0.7 | 21 ± 0.8 |
| | | | | | −11.9 ± 0.6 | 208 | 23 ± 0.9 | 32 ± 1.5 | 24 ± 0.7 | 22 ± 0.8 |
| K1W | 13740 | 14.1 ± 0.3 | −19.5 ± 1.1 | 274 | −9.9 ± 0.5 | 209 | 18 ± 0.9 | 32 ± 1.2 | 26 ± 0.4 | 23 ± 0.6 |
| | | | | | −9.4 ± 0.3 | 209 | 17 ± 0.9 | 33 ± 1.2 | 26 ± 0.5 | 23 ± 0.6 |
| F8W | 13721 | 13.6 ± 0.6 | −23.2 ± 1.4 | 275 | −11.0 ± 0.5 | 208 | 20 ± 0.7 | 31 ± 1.2 | 25 ± 0.5 | 22 ± 0.6 |
| | | | | | −10.6 ± 0.8 | 209 | 19 ± 0.8 | 34 ± 1.2 | 25 ± 0.5 | 22 ± 0.7 |
| D38W | 13753 | 16.9 ± 0.1 | −23.0 ± 1.4 | 276 | −11.2 ± 0.5 | 208 | 19 ± 0.9 | 34 ± 1.4 | 24 ± 0.6 | 22 ± 0.8 |
| | | | | | −10.8 ± 0.5 | 208 | 17 ± 0.8 | 37 ± 1.4 | 24 ± 0.6 | 21 ± 0.8 |
| Y73W | 13705 | 13.1 ± 0.1 | −19.6 ± 1.3 | 274 | −12.4 ± 0.3 | 208 | 21 ± 0.6 | 33 ± 1.1 | 24 ± 0.6 | 22 ± 0.6 |
| | | | | | −12.4 ± 0.3 | 207 | 21 ± 0.7 | 32 ± 1.2 | 25 ± 0.5 | 23 ± 0.7 |
| Y76W | 13705 | 13.3 ± 0.3 | −28.5 ± 0.6 | 276 | −11.3 ± 0.2 | 208 | 20 ± 0.8 | 33 ± 1.4 | 25 ± 0.5 | 21 ± 0.7 |
| | | | | | −11.1 ± 0.2 | 207 | 18 ± 0.8 | 35 ± 1.4 | 25 ± 0.7 | 21 ± 0.8 |
| Y92W | 13705 | 14.7 ± 0.3 | 3.0 ± 0.3 | 289 | −13.3 ± 0.5 | 208 | 23 ± 1.0 | 34 ± 1.7 | 24 ± 0.8 | 20 ± 0.9 |
| | | | | | −12.0 ± 0.3 | 209 | 21 ± 0.9 | 33 ± 1.6 | 25 ± 0.7 | 21 ± 0.8 |
| K104W | 13740 | 14.0 ± 0.1 | −34.5 ± 0.5 | 275 | −11.4 ± 0.4 | 208 | 22 ± 0.8 | 32 ± 1.4 | 24 ± 0.7 | 22 ± 0.8 |
| | | | | | −10.7 ± 0.1 | 209 | 19 ± 0.8 | 34 ± 1.3 | 25 ± 0.6 | 22 ± 0.7 |
| Y115W | 13705 | 13.0 ± 0.2 | −22.1 ± 0.5 | 283 | −11.7 ± 0.2 | 209 | 21 ± 0.9 | 35 ± 1.5 | 24 ± 0.7 | 20 ± 0.8 |
| | | | | | −11.3 ± 0.2 | 209 | 20 ± 0.8 | 35 ± 1.5 | 24 ± 0.7 | 20 ± 0.8 |
| V124W | 13765 | 13.1 ± 0.3 | −37.8 ± 1.1 | 275 | −10.1 ± 0.3 | 208 | 20 ± 0.7 | 35 ± 1.3 | 24 ± 0.6 | 21 ± 0.7 |
| | | | | | −10.4 ± 0.3 | 208 | 20 ± 0.7 | 33 ± 1.2 | 25 ± 0.6 | 22 ± 0.7 |
| mean | | | | | −11.4 ± 1.0 | | 20.6 ± 1.5 | 33.6 ± 1.1 | 24.3 ± 0.7 | 21.5 ± 1.0 |
| | | | | | −11.1 ± 0.9 | | 19.5 ± 1.9 | 33.8 ± 1.5 | 24.8 ± 0.6 | 21.7 ± 0.9 |

[a] For each protein, as well as for the mean values in columns 6−11, the first line pertains to 20 °C and the second line to 20 °C after heating to 80 °C and then cooling to 20 °C. The mean values are averages over both the wild-type and mutant proteins. [b] Molecular weight, computed from the amino acid composition. [c] Extinction coefficient ($\times 10^3$ $M^{-1}$ $cm^{-1}$) at the maximum of the absorption spectrum (at a wavelength of 278 nm). [d] [Θ] and $[\Theta]_m$ represent the molar ellipticity and mean residue molar ellipticity in kilodegrees × square centimeter per decimole at the minimum of the CD spectrum at $\lambda$ and $\lambda_m$, respectively. [e] α, $\beta$, and turn represent the relative amount of amino acid residues involved in α-helices, $\beta$-sheets, and $\beta$-turns, respectively; $r$ (=1 − α − $\beta$ − turn) is the remainder. The errors pertain to the fittings according to the Provencher−Glöckner procedure (*38*−*40*), and not to errors in the determination of molar ellipticity.

of the experiments carried out at 80 °C.

UV absorption spectra were measured with a model 17DS UV−vis−IR spectrophotometer (Aviv Associates) and corrected for Rayleigh light scattering by the procedure of Leach and Scheraga (*43*). The extinction coefficients of the mutants were determined relative to the standard wild-type value of $9.8 \times 10^3$ $M^{-1}$ $cm^{-1}$ (*44*) using the concentrations obtained by the Biuret method (*45*). The extinction coefficients of the nine mutants were higher than that of wild-type RNase A, reflecting the contribution of added tryptophan. These extinction coefficients generally fall in the range of 13−14 $\times 10^3$ (Table 1); however, the value for the D38W mutant is unusually high ($16.9 \times 10^3$), possibly reflecting an interaction between W38 and Y92.

Steady-state fluorescence measurements were taken at 20 °C, using an AT-105 spectrofluorimeter (Aviv Associates) and quartz cells with a 1.0 cm × 1.0 cm cross section. The excitation wavelength was set to 297 nm (bandwidth of 1−2 nm), and the emitted fluorescence spectra were resolved to 1.0 nm after correcting for the spectral sensitivity of the spectrofluorimeter. The quantum yield, $q$, was determined by using a standard aqueous solution of tryptophan at 20 °C, for which $q = 0.20$ (*46*, *47*, *71*). The optical density of all solutions was adjusted to 0.04−0.11 at 297 nm.

Time-resolved fluorescence measurements were taken at 22 °C (with laser excitation at 297 nm and emission at 350 ± 8 nm) by using a single photon-counting system described elsewhere (*48*). The data were then fit to a sum of exponentials using a least-squares analysis.

*Thermal Transition Experiments.* Thermal transition measurements were carried out at pH 5.0 by varying the temperature from 20 to 80 °C in increments of 1−2 °C, while monitoring the ellipticity at 215 nm, the absorption at 278 nm, and the steady-state tryptophan fluorescence spectra. The temperatures were controlled to within 0.1 °C. After each target temperature had been reached, the solutions were allowed to equilibrate for 1.5−2 min (for far-UV CD measurements) or 2−3 min (for near-UV CD, absorption, and fluorescence measurements). Prior to all spectroscopic measurements, the protein solutions were aspirated under vacuum and their concentrations were measured spectrophotometrically.

*Thermal Transitions Are Reversible under These Conditions.* The thermal transitions followed by far-UV CD, by UV absorption, and by fluorescence were found to be reversible for all mutants, which is consistent with previous studies (*1*−*12*). The irreversibility of thermal denaturation above pH 7 (*2*) arises primarily from succinimide formation at the Asn-67−Gly-68 peptide bond (*49*). This succinimide formation occurs primarily at higher pH, and only if the protein is held at a higher temperature (>80 °C) for some time. The experiments presented here were carried out at pH 5, well below the pH threshold for irreversibility.

The folding equilibrium constant $K_u$ for the thermal transition was computed as

$$K_u = \frac{\xi - \xi_N}{\xi_U - \xi} \quad (1)$$

where $\xi$ represents the measured signal (UV CD or UV absorbance) and $\xi_N$ and $\xi_U$ represent the corresponding values of the pure folded and unfolded states, respectively, under the solution conditions of the measurement.

Table 2: Specific Activity of the Trp Mutants Relative to the Activity of the Wild-Type Protein

| mutant[a] | activity (%) | mutant[a] | activity (%) |
|---|---|---|---|
| wild type | 100 | Y76W | 86 ± 7 |
| K1W | 94 ± 5 | Y92W | 85 ± 6 |
| F8W | *b* | K104W | 94 ± 5 |
| D38W | *b* | Y115W | 85 ± 7 |
| Y73W | 92 ± 10 | V124W | 95 ± 6 |

[a] Each mutant protein contains one tryptophan residue. [b] No enzymatic activity was found for these mutants.

The values of $\xi_N$ and $\xi_U$ for the thermal transitions measured by UV absorbance and far-UV CD were obtained by assuming that the spectroscopic signals for the pure folded and unfolded states vary linearly with the temperature, i.e., $\xi_N = a_N + b_N t$ and $\xi_U = a_U + b_U t$, where $a$ and $b$ are constants and $t$ represents the temperature in degrees Celsius. These $a$ and $b$ parameters were determined for the folded and unfolded state by fitting the spectroscopic data in a small range at the extremes, i.e., at low and high temperatures, respectively. In contrast, the tryptophan fluorescence signals of the folded and unfolded states were assumed to vary linearly with $T/\eta$ (where $T$ is the absolute temperature and $\eta$ the viscosity), i.e., $\xi_N = a_N + b_N(T/\eta)$ and $\xi_U = a_U + b_U(T/\eta)$, where $\xi = q_{20}/q$, the inverse quantum yield normalized to its value at 20 °C. The solution values of $\eta$ at different temperatures were taken to be equal to those of pure water (*50*); presumably, the low protein concentration (~0.7 mg/mL) makes a negligible contribution to the viscosity, whether unfolded or not. The values of $\ln K_u$ were fitted to the following equation

$$R \ln K_u = a - b/T \quad (2)$$

where $R$ is the gas constant (1.987 cal/mol) and the slope $b$ and intercept $a$ correspond to the van't Hoff enthalpy $\Delta H$ and entropy $\Delta S$ of unfolding, respectively. The midpoint temperature of the transition was determined as $T_m = b/a$.

## RESULTS

*Wild-Type RNase A Control Experiments.* The wild-type data agree with previously published data insofar as these are available. The extinction coefficient (Table 1) and enzymatic activity (Table 2) agree with those published previously (*44*). The far-UV spectra (Figure 2) agreed with previously published spectra (*9*, *20*, *51*−*53*), and the secondary structure contents estimated from these data also agree with the accepted percentages known from the crystal structure (*33*). The near-UV CD spectrum measured at 20 °C and pH 5.0 (Figure 3) was closely similar to spectra measured at room temperature and neutral pH (*52*, *54*−*56*). Finally, the thermal transition temperature and fitted thermodynamic parameters agreed with those calculated previously (*3*, *12*) for the wild-type protein under similar conditions.

*The Trp Mutants Have Native-like Structure at 20 °C.* Seven of the nine Trp mutants exhibit high specific enzymatic activity (Table 2), which is strong evidence that their folded structure is highly similar to that of the wild-type protein. The sole exceptions are F8W and D38W for which no

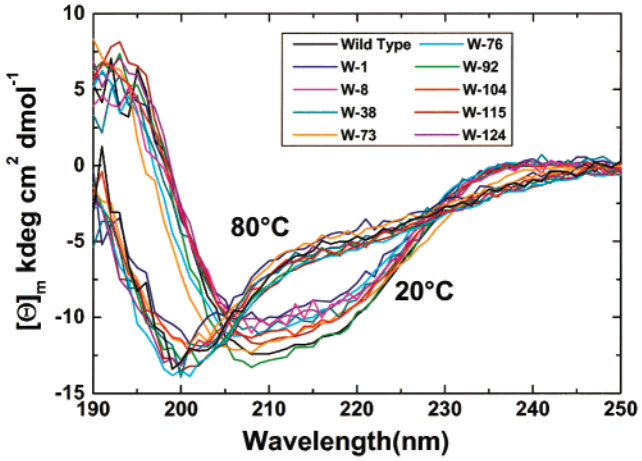


FIGURE 2: Equilibrium far-UV CD spectra of wild-type RNase A and the nine tryptophan mutants recorded at 20 and 80 °C and pH 5.0. The minimal values of each spectrum correspond to the $[\Theta]_m$ values in Table 1 (column 6) and Table 3 (column 2).

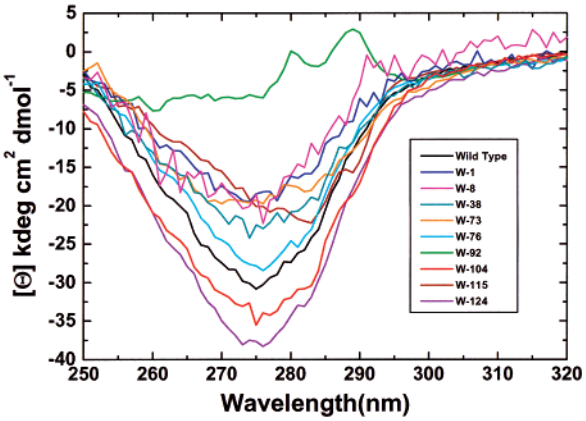


FIGURE 3: Equilibrium near-UV circular dichroism spectra of wild-type RNase A and the nine tryptophan mutants recorded at 20 °C and pH 5.0. The minimal values of each spectrum correspond to the [Θ] values in Table 1 (column 4).

enzymatic activity was found. However, the absence of enzymatic activity is likely due to the fact that these two residues are close to the active site (i.e., close to His-12 and Lys-41, respectively) and minor structural perturbations can affect the activity.

The far-UV CD spectra of the mutants agree closely with that of the wild-type protein at 20 °C (Figure 2). Since such spectra are believed to report on the secondary structure of the protein, this agreement suggests that all nine of the Trp mutants adopted a native-like fold. To support this conclusion further, the secondary structure contents of the nine mutants were estimated from the far-UV CD spectra at 20 °C (Table 1). The results agree with the secondary structure content of the wild-type protein, consistent with a native-like structure for the nine tryptophan mutants.

*The Trp Mutations Induce Local Structural Changes.* Near-UV CD spectra taken at 20 °C (Figure 3) exhibit more variation among the mutants than do the far-UV CD spectra (Figure 2). In general, near-UV CD spectra are believed to report on the local asymmetric environment of aromatic residues; thus, these spectra suggest that the details of the tertiary packing differ among the nine Trp mutants. This interpretation is structurally plausible and consistent with the thermal transition data reported below, which exhibit different thermal transition temperatures and enthalpies for the nine mutants.

The near-UV CD spectra can be grouped into three families (Figure 3). The Y76W, K104W, and V124W mutants have spectra very similar to that of wild-type RNase A. In contrast, the K1W, F8W, D38W, Y73W, and Y115W mutants exhibit spectra that are similar in shape but significantly reduced in amplitude compared to that of the wild-type protein. Finally, the Y92W mutant is anomalous, with no resemblance to the wild-type protein; rather, this protein exhibits a small positive peak, which may correspond to the 0−0 $^1L_b$ electronic transition observed at lower frequencies in the wild-type protein and other mutants. It is remarkable that the mutation of a single tyrosine (of six in wild-type RNase A) is capable of altering the near-UV CD spectrum so drastically, especially since this mutation occurs in a highly flexible loop and does not appear to alter the native structure. The fluorescence anisotropy of Trp-92 indicates restricted rotational freedom due to interactions with the protein environment (*57*). This may reflect a ring−ring interaction between Trp-92 and Pro-93 that has been observed in peptide analogues (unpublished results) and that has been hypothesized to account for the large fluorescence burst phase observed in single-jump refolding studies of this mutant (*32*).

It has been hypothesized that interactions between Tyr-73 and Tyr-115 are primarily responsible for the near-UV CD band observed in wild-type RNase A (*58*). The side-chain hydroxyl groups of these tyrosines appear to be involved in a medium-strength hydrogen bond, as observed both crystallographically (*33*) and by Raman spectroscopy (*27*, *31*). We note, however, that the tryptophan mutations of these residues result in relatively modest changes in this band. Therefore, a specific structural interpretation of this band remains in doubt [the minima of those mutants are shifted toward a higher wavelength compared to those of the other mutants (about 283 nm compared to about 275 nm in the other mutants excluding W-92)].

*Residual Structure Persists at High Temperatures.* The similar far-UV CD spectra observed for the wild-type and mutant proteins at 80 °C do not correspond to a statistical coil, suggesting that some structure may be present (Figure 2). (We denote this structure as "residual", since it is likely that it consists of structural components of the native protein; however, in principle, nonnative structure is also possible.) The secondary structure contents for all the mutant and wild-type proteins at 80 °C (Table 3) suggest that residual structure is found in ∼35−45% of the ensembles of denatured wild-type and mutant proteins, and that the tryptophan substitutions do not alter the residual structure significantly.

Earlier studies have also indicated the presence of residual structure in the thermally denatured protein (*10*, *16*, *23*, *27*, *59*−*61*). Taken together, these accumulated data represent strong evidence that contradicts a strict two-state model for thermal unfolding. Presumably, the statistical distribution of conformations in *unfolded* states may vary significantly with solution conditions.

*Multiple Transitions Are Observed during Heating.* Consistent with the native fold and small structural disruptions observed by far- and near-UV CD, respectively, the nine mutants all exhibited a stability slightly lower than that of wild-type RNase A, as judged by the approximately 2.5−

Table 3: Parameters of the Far-UV CD Spectra and Secondary Structure of Wild-Type RNase A and of Tryptophan Mutants at pH 5 and 80 °C[a]

| mutant | $[\Theta]_m$ | $\lambda_m$ (nm) | α (%) | β (%) | turn (%) | *r* (%) |
|---|---|---|---|---|---|---|
| wild type | −13.0 ± 0.6 | 200 | 10 ± 0.2 | 19 ± 0.5 | 16 ± 0.3 | 54 ± 0.6 |
| K1W | −11.8 ± 0.8 | 201 | 12 ± 0.4 | 10 ± 0.7 | 13 ± 0.4 | 66 ± 0.8 |
| F8W | −11.4 ± 0.8 | 200 | 10 ± 0.5 | 18 ± 0.9 | 16 ± 0.7 | 56 ± 1.2 |
| D38W | −12.0 ± 0.5 | 200 | 9 ± 0.3 | 15 ± 0.5 | 14 ± 0.3 | 62 ± 0.6 |
| Y73W | −13.5 ± 0.7 | 200 | 10 ± 0.3 | 13 ± 0.6 | 13 ± 0.4 | 64 ± 0.8 |
| Y76W | −13.7 ± 0.6 | 200 | 10 ± 0.3 | 12 ± 0.6 | 12 ± 0.4 | 66 ± 0.7 |
| Y92W | −13.0 ± 0.5 | 201 | 10 ± 0.3 | 13 ± 0.5 | 13 ± 0.3 | 64 ± 0.6 |
| K104W | −11.4 ± 0.3 | 201 | 10 ± 0.3 | 15 ± 0.5 | 14 ± 0.3 | 61 ± 0.6 |
| Y115W | −13.2 ± 0.4 | 201 | 10 ± 0.3 | 13 ± 0.6 | 13 ± 0.4 | 64 ± 0.8 |
| V124W | −13.2 ± 0.2 | 200 | 9 ± 0.2 | 13 ± 0.5 | 13 ± 0.3 | 64 ± 0.6 |
| mean | −12.6 ± 0.9 | | 10.0 ± 0.8 | 14.1 ± 2.7 | 13.7 ± 1.3 | 62.1 ± 4.1 |

[a] For definitions of the parameters, see Table 1.

Table 4: Midpoint Temperature (in degrees Celsius) and van't Hoff Enthalpy (kilojoules per mole) of the Main Thermal Transition of wt-RNase A and the Trp Mutants Detected by Far-UV CD (CD), UV Absorbance (UV), and Tryptophan Fluorescence (TF) at pH 5.0

| | CD | | UV | | TF | |
|---|---|---|---|---|---|---|
| mutant | $T_m$ | Δ*H* | $T_m$ | Δ*H* | $T_m$ | Δ*H* |
| wild type | 64.3 ± 0.1 | 380 ± 45 | 58.2 ± 0.2 | 426 ± 20 | – | – |
| K1W | 67.6 ± 0.1 | 347 ± 35 | 60.0 ± 0.2 | 272 ± 8 | – | – |
| F8W | 55.4 ± 0.2 | 309 ± 54 | 48.1 ± 0.1 | 317 ± 17 | 46.8 ± 0.1 | 203 ± 12 |
| D38W | 60.8 ± 0.2 | 248 ± 19 | 55.4 ± 0.2 | 321 ± 43 | 59.0 ± 0.2 | 302 ± 7 |
| Y73W | 61.8 ± 0.1 | 338 ± 83 | 52.1 ± 0.3 | 296 ± 30 | 57.3 ± 0.2 | 315 ± 38 |
| Y76W | 58.2 ± 0.2 | 134 ± 5 | 52.7 ± 0.2 | 274 ± 33 | 56.8 ± 0.1 | 251 ± 1.1 |
| Y92W | 65.4 ± 0.1 | 254 ± 18 | 60.7 ± 0.2 | 395 ± 7 | 59.4 ± 0.2 | 315 ± 67 |
| K104W | 53.4 ± 0.1 | 268 ± 16 | 48.9 ± 0.8 | 406 ± 14 | 42.4 ± 0.1 | 439 ± 9 |
| Y115W | 59.9 ± 0.2 | 180 ± 6 | 54.2 ± 0.2 | 203 ± 10 | 50.3 ± 0.1 | 311 ± 8 |
| V124W | 59.8 ± 0.2 | 272 ± 45 | 55.2 ± 0.1 | 378 ± 11 | 61.3 ± 0.1 | 386 ± 38 |

11 °C shifts in the transition midpoint temperature $T_m$ (Table 4); the corresponding van't Hoff enthalpies are also given in Table 4.

Remarkably, the van't Hoff plots of the thermal unfolding monitored by tyrosine absorbance and far-UV CD spectra (discussed in detail below) indicated the presence of at least two conformational transitions. For nearly all of the mutants, there is a pronounced kink in the van't Hoff plots, which cannot be fit well by assuming a single transition. One transition corresponds to the main cooperative unfolding transition near 60 °C, but the other generally occurs at a significantly lower temperature, in the range of 30−45 °C.

The observation of multiple thermal transitions is consistent with earlier studies showing conformational transitions that occur at temperatures far lower than that of the main cooperative unfolding transition. The earliest such studies were proteolytic, and indicated that a conformational transition occurred in the range of 30−45 °C, which led to the proteolytic susceptibility of the second helix (residues 25−35) and to the end of the main β-sheet, notably in the vicinity of Phe-46 and Met-79 (*15*). Later studies also showed that conformational transitions occurred in this range near His-105 and in the N-terminal helix (*16*, *18*, *70*). These regions are contiguous in the native structure, with the N-terminal helix nestling between the second helix, the end of the main β-sheet, and the C-terminal β-hairpin; thermal destabilization of one of these structures could destabilize all of them. However, other data showed no significant structural or energetic changes, e.g., in the overall dimensions of the protein (*60*), in its backbone topology (CD data), in its heat absorption (*3*), and in the strong hydrogen bond between Asp-14 of helix I and Tyr-25 of helix II (*27*, *31*, *59*). Therefore, the conformational transition must be relatively subtle and entropically favored, e.g., a loosening of the packing of the major hydrophobic core composed of the C-terminal β-hairpin and the N-terminal helix. This hypothesis of a quasi-molten-globule transition in the pretransition region is supported by the fluorescence data reported below.

The presence of residual structure at 80 °C and of pretransitional changes in the statistical distribution of folded conformations suggests that a strict two-state model does not accurately describe the thermal unfolding of RNase A. Accordingly, the following sections describe tryptophan fluorescence studies that were carried out to characterize both the residual structure ensemble of the thermally unfolded state and the nature of the conformational transitions that precede the global unfolding of RNase A.

*Steady-State Tryptophan Fluorescence: Emission Maxima and Quantum Yields.* Fluorescence spectra were collected for the nine tryptophan mutants at 20 and 80 °C and again at 20 °C (Table 5 and Figure 4). In all mutants, the final fluorescence spectrum agreed with the initial spectrum to within experimental error, indicating that the thermal transition was fully reversible. As a control, a spectrum was also collected for free, unblocked tryptophan at 20 °C.

In four mutants, the emission maxima of the fluorescence spectra were shifted significantly toward longer wavelengths at higher temperatures; such shifts are known to correspond to an increase in the effective dielectric constant of the medium corresponding to a more polar environment surrounding the tryptophan residue (*47*). The largest shift occurred for the F8W mutant, from ∼331 to 350 nm, consistent with the full burial of F8 in the native structure. Smaller shifts were observed for the Y73W, Y92W, and V124W mutants, consistent with the fact that all of these residue positions are partially buried in the native structure.

Table 5: Parameters of Tryptophan Fluorescence of RNase A Tryptophan Mutants in Sodium Acetate Buffer (pH 5.0)

| mutant | temperature (°C) | $q^a$ (%) | $\lambda_{max}{}^b$ (nm) |
|---|---|---|---|
| free tryptophan | 20 | 20[c] | 353[c] |
| K1W | 20 | 7.69 ± 0.13 | 344 |
| | 80 | 2.45 ± 0.06 | 344 |
| | 20 ← 80[d] | 7.31 ± 0.16 | 343 |
| F8W | 20 | 8.70 ± 0.15 | 331 |
| | 80 | 5.83 ± 0.14 | 350 |
| | 30 ← 80 | 8.92 ± 0.20 | 335 |
| D38W | 20 | 16.18 ± 0.16 | 329 |
| | 80 | 4.75 ± 0.08 | 331 |
| | 20 ← 80 | 16.15 ± 0.16 | 329 |
| Y73W | 20 | 0.57 ± 0.02 | 334 |
| | 80 | 0.85 ± 0.02 | 343 |
| | 20 ← 80 | 0.63 ± 0.02 | 334 |
| Y76W | 20 | 16.34 ± 0.12 | 337 |
| | 80 | 3.45 ± 0.05 | 334 |
| | 20 ← 80 | 16.15 ± 0.13 | 336 |
| Y92W | 20 | 2.76 ± 0.04 | 332 |
| | 80 | 2.41 ± 0.04 | 341 |
| | 20 ← 80 | 2.89 ± 0.04 | 333 |
| K104W | 20 | 10.27 ± 0.10 | 342 |
| | 80 | 3.38 ± 0.05 | 342 |
| | 20 ← 80 | 10.27 ± 0.10 | 343 |
| Y115W | 20 | 2.83 ± 0.03 | 334 |
| | 80 | 4.23 ± 0.06 | 337 |
| | 20 ← 80 | 3.10 ± 0.04 | 334 |
| V124W | 20 | 4.73 ± 0.06 | 342 |
| | 80 | 2.94 ± 0.05 | 349 |
| | 20 ← 80 | 4.81 ± 0.07 | 341 |

[a] Quantum yield. [b] Maximum wavelength of the spectrum determined with an accuracy of 1 nm. [c] From refs *46*, *47*, and *71*. [d] After heating to 80 °C and then cooling to 20 °C.

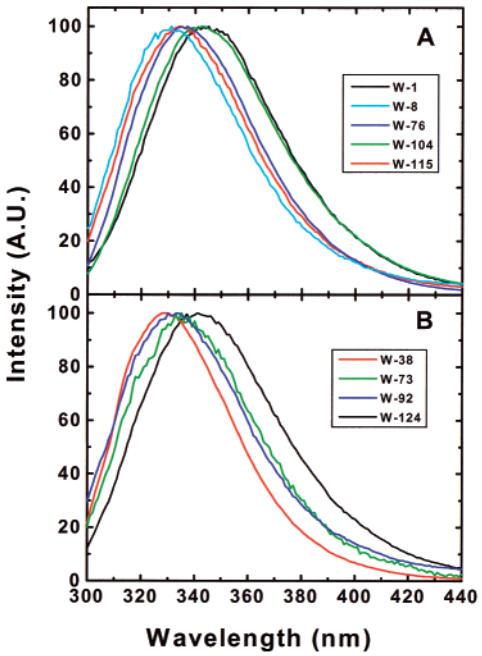


FIGURE 4: Equilibrium tryptophan fluorescence spectra of the nine tryptophan mutants recorded at 20 °C (wild-type RNase A has no tryptophan). The excitation wavelength was 297 nm, with a spectral resolution of 1 nm. The spectra are normalized to their maximum intensity.

In contrast, very small shifts (within the experimental error) were observed for the K1W, D38W, Y76W, K104W, and Y115W mutants; these residue positions are more exposed to the solution on the surface of the protein in the native wild-type structure. The small shifts in the fluorescence emission maxima of these surface-exposed residues suggest that the dielectric environment of these residues is really identical in the native and thermally unfolded states.

Table 6: Parameters of Time-Resolved Tryptophan Fluorescence of RNase A Trp Mutants[a] at pH 5.0 and 22 °C

| mutant | $\tau_1$ (ns) | $\alpha_1$ | $\tau_2$ (ns) | $\alpha_2$ | $\tau_3$ (ns) | $\alpha_3$ | $\chi^2$ | $\tau_{av}$ (ns) |
|---|---|---|---|---|---|---|---|---|
| K1W | 0.38 | 0.43 | 1.32 | 0.50 | 3.99 | 0.06 | 1.15 | 1.08 |
| F8W | 0.23 | 0.23 | 1.09 | 0.44 | 2.41 | 0.33 | 1.12 | 1.32 |
| D38W | 0.85 | 0.10 | 2.32 | 0.90 | – | – | 1.15 | 2.18 |
| Y73W | 0.13 | 0.52 | 0.89 | 0.33 | 2.62 | 0.15 | 1.06 | 0.77 |
| Y76W | 0.92 | 0.34 | 2.97 | 0.62 | 6.51 | 0.04 | 1.31 | 2.42 |
| Y92W | 0.067 | 0.91 | 0.75 | 0.06 | 2.73 | 0.03 | 1.03 | 0.185 |
| K104W | 0.18 | 0.29 | 1.20 | 0.41 | 3.90 | 0.30 | 1.28 | 1.71 |
| Y115W | 0.097 | 0.71 | 0.66 | 0.24 | 3.14 | 0.05 | 1.14 | 0.39 |
| V124W | 0.08 | 0.74 | 1.44 | 0.20 | 3.87 | 0.06 | 1.54 | 0.59 |

[a] $\tau$ is the lifetime. $\alpha_i$ is the contribution of component $i$ to the total fluorescence intensity. $\tau_{av}$ is the averaged lifetime, computed as $\Sigma_i\alpha_i\tau_i/\Sigma_i\alpha_i$.

Interestingly, the emission maxima of the five surface-exposed mutants are lower than that of the unblocked tryptophan standard ($\lambda_m = 353$ nm). In particular, the D38W, Y76W, and Y115W mutants all had emission maxima in the range of 329−337 nm even at 80 °C. Moreover, the fully buried F8W mutant had an emission maximum of 331 nm at 20 °C, a value very similar to those of the mutants with tryptophans inserted into surface-exposed residue positions of wild-type RNase A. The relatively low fluorescence emission maxima of these mutants (compared to free solvent-exposed tryptophans) may reflect an unusually hydrophobic local environment of these tryptophans, possibly due to adjacent residues or to residual structure that survives denaturation. In particular, tryptophans 76 and 115 belong to the major hydrophobic core, and there is evidence that some hydrophobic interactions in this core region survive thermal denaturation (*15*). In contrast, D38W may form aromatic−aromatic interactions with residues Tyr-92 and Tyr-97; these residues are effectively adjacent, because of the disulfide bond between residues 40 and 95. A W38−Y92 interaction is also suggested by the anomalously high molar absorbance of the D38W mutant (Table 1).

The fluorescence quantum yields of the tryptophan residues also depend on the local environment and vary from 16 to 0.6% at 20 °C (Table 5). The variation of the Trp fluorescence quantum yield reflects a variation in both the nonspecific quenching by solvent molecules and the specific quenching by local interactions of charged side chains, carbonyls, and sulfur-containing functional groups (*47*).

The variation of the fluorescence quantum yields did not correlate with the positions of the emission maximum. This is another indication of specific local interactions that can be changed upon unfolding depending on whether the side chains are involved in local (e.g., Trp-38) or nonlocal (e.g., Trp-92) interactions.

*Tryptophan Fluorescence: Quantum Yields and Mean Lifetimes.* Time-resolved fluorescence measurements were also taken for these nine mutants at 22 °C. The fluorescence of all tryptophan mutants exhibited triphasic exponential decays, with the exception of the D38W mutant, for which only a biphasic decay could be resolved (Table 6).

The mean fluorescence lifetimes ($\tau_{av}$) of the mutants were strongly positively correlated with their quantum yields (Figure 5), which is consistent with the fundamental equation

Table 7: Parameters for the Dependence of the Reciprocal Quantum Yield of Tryptophan Fluorescence of the RNase A Tryptophan Mutants on the Temperature/Viscosity Ratio in the Native and Temperature-Induced Unfolded States (see eq 3)

| | native state | | | unfolded state | | |
|---|---|---|---|---|---|---|
| mutant | slope $b_n$ ($\times 10^3$ cP/deg) | intercept, $a_n$ | $r^a$ | slope $b_u$ ($\times 10^3$ cP/deg) | intercept, $a_u$ | $r^a$ |
| V124W | 0.68 ± 0.06 | 0.79 ± 0.02 | 0.997 | 1.69 ± 0.11 | −0.17 ± 0.10 | 0.999 |
| F8W | 1.11 ± 0.01 | 0.67 ± 0.01 | 0.999 | 1.61 ± 0.01 | −0.11 ± 0.01 | 0.999 |
| D38W | 1.17 ± 0.07 | 0.65 ± 0.02 | 0.998 | 2.22 ± 0.07 | 0.49 ± 0.07 | 0.999 |
| Y73W | 1.12 ± 0.13 | 0.66 ± 0.05 | 0.993 | 0.82 ± 0.11 | 0.10 ± 0.10 | 0.999 |
| Y92W | 0.94 ± 0.12 | 0.72 ± 0.04 | 0.996 | 1.17 ± 0.14 | 0.11 ± 0.13 | 0.999 |
| mean | 1.07 ± 0.09 | 0.67 ± 0.02 | | | | |
| Y76W | 1.32 ± 0.04 | 0.60 ± 0.02 | 0.996 | 3.65 ± 0.09 | 0.32 ± 0.08 | 0.999 |
| K104W | 1.44 ± 0.09 | 0.57 ± 0.03 | 0.998 | 3.56 ± 0.07 | 0.19 ± 0.05 | 0.996 |
| Y115W | 1.53 ± 0.06 | 0.56 ± 0.02 | 0.998 | 0.52 ± 0.06 | 0.09 ± 0.05 | 0.992 |
| mean | 1.43 ± 0.11 | 0.58 ± 0.02 | | | | |

[a] $r$ is the correlation coefficient of the linear regression. The values of the slope and intercept in eq 3 were normalized by the reciprocal quantum yield at 20 °C and pH 5.0.

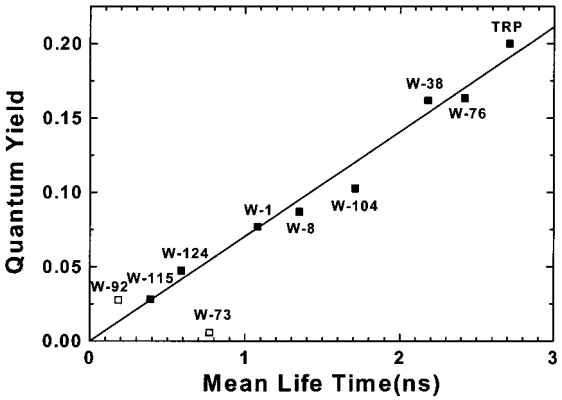


FIGURE 5: Plot of quantum yield vs mean lifetime for the tryptophan fluorescence of the nine tryptophan mutants of RNase A in the native state. The linear fit agrees with data taken for other proteins and for free tryptophan, suggesting that most of the tryptophans in the nine mutants are quenched by solvent interactions. However, the Y92W and Y73W mutants are anomalous, suggesting that other mechanisms contribute to their quenching.

$q = \tau/\tau_r$, where $\tau_r$ is the radiative lifetime. The fitted common value for $\tau_r$ was 14 ns for seven of the mutants (excluding Y73W and Y92W), which falls within the range of 10−20 ns found for other proteins containing tryptophan (*46*, *71*), and is also consistent with the radiative lifetime of tryptophan in water, ∼16 ns (*62*). These observations are consistent with a model in which the substituted tryptophans are quenched primarily by the solvent.

The tryptophan residue of mutant Y73W did not conform to the correlation between $q$ and $\tau_{av}$ (Figure 5). Tryptophan 73 had an exceptionally low quantum yield (Table 5), while $\tau_{av}$ was not reduced proportionally. This is an indication of the presence of a subpopulation which is ground-state-quenched. Tryptophan 73 is close to the disulfide bond between residues 65 and 72, which may account for this efficient quenching. Disulfide bonds are known to be effective quenchers of Trp fluorescence caused by an enhancement of nonradiative intersystem crossing to triplet states. Since this tryptophan residue is adjacent to the disulfide bond along the backbone, it seems likely that this quenching mechanism would also be operative in the denatured state. Tryptophan 92 has a very short fluorescence lifetime (Table 6), probably as a result of efficient collisional quenching by the disulfide bond between residues 40 and 95.

*Tryptophan Fluorescence: Temperature Dependence of the Quantum Yields.* In the absence of conformational transitions, the reciprocal quantum yield, $1/q$, is a linear function of the absolute temperature, $T$, corrected for the viscosity, $\eta$, which reflects a trivial temperature quenching mechanism: $1/q = a + b(T/\eta)$ (*63*, *64*). This equation is applicable for single-chromophore proteins such as the Trp mutants considered here, and accounts for diffusion processes in the solvent which control the mobility of the internal residues in a protein molecule and the collisional quenching by the solvent. The $a$ term is a temperature-independent sum of the excited-state deactivation rate constants at a temperature of absolute zero, or infinite viscosity (both of which imply no temperature-related motion). It probably represents intrinsic local quenching interactions such as the interaction of a tryptophan with a spatially adjacent disulfide bond. The slope $b$ has been interpreted as a temperature-independent index of mobility and is meant to reflect the frequency of quenching interactions that occur with the solvent or with other protein groups.

To allow comparisons between the mutants whose quantum yields differ dramatically (Table 5), we transformed the above equation as

$$\frac{q_{20}}{q} = a + b\left(\frac{T}{\eta}\right) \qquad (3)$$

where $q_{20}$ represents the quantum yield at 20 °C, which is introduced as a normalization factor.

The thermal transition plots of $q_{20}/q$ (Figure 6) fit well in the temperature regimes where the folded or the unfolded states are populated almost exclusively, supporting the validity of using the tryptophan quenching relationship in eq 3 to describe the following process in RNase A. These plots also resemble analogous plots made for other proteins (*65*, *66*). The fitting of the quantum yields for the pure native and unfolded states allows an unfolding equilibrium constant $K_u$ to be defined on the basis of these linear fits in a manner analogous to that which is used to obtain $K_u$ from far-UV CD and UV absorption data in this study. First, from the wide variation in the slopes of the $q_{20}/q$ plots for the different tryptophan mutants in the thermally unfolded state, it is evident that the tryptophans are not quenched equally by the solvent, suggesting different degrees of solvent exposure in the thermally unfolded states of the mutants. Second, Figure

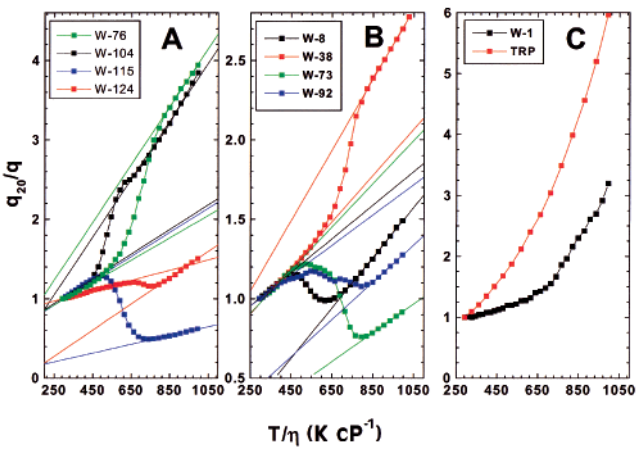


FIGURE 6: Dependence of reciprocal relative quantum yield $q_{20}/q$ on absolute temperature, corrected for the viscosity change, $T/\eta$, for the tryptophan mutants of RNase A in 0.01 M sodium acetate buffer (pH 5.0, room temperature). The positions of the substituted tryptophan residues are indicated in the panels. Straight lines show the best fit (least-squares) linear regressions.

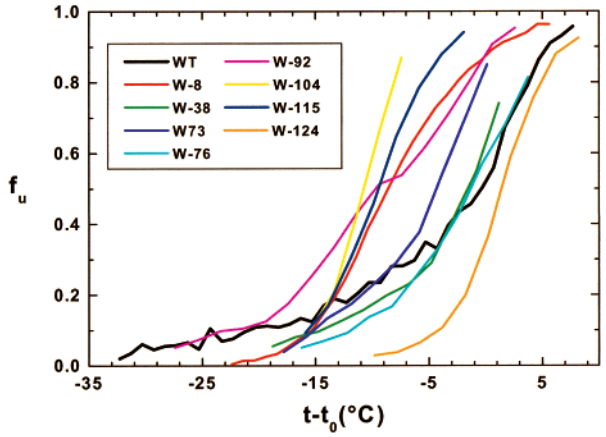


FIGURE 7: Fraction $f_u$ of the population of the unfolded state in the tryptophan fluorescence-detected thermal unfolding of the tryptophan mutants of RNase A as a function of the temperature expressed as the difference between the current temperature $T$ and the midpoint temperature $T_m$ of the thermal unfolding of the same mutants detected by far-UV CD. The K1W mutant shows no fluorescence-detected transition.

6 also makes evident the fact that the cooperative unfolding transitions of some tryptophan mutants occur at a much lower temperature than the main cooperative unfolding transition, e.g., the transitions of F8W and K104W, in agreement with the pretransition data cited above for His-105 and for the N-terminal helix (*16*, *18*, *70*). These two topics are discussed in turn.

*Differential Solvent Exposure in the Thermally Unfolded State.* The quantum yield plots of Figure 6 show cooperative transitions occurring in the vicinity of the various substituted tryptophan residues. The temperatures at which the local transitions occur and their relation to the transition temperature of the global cooperative unfolding transition will be discussed in the following section. At temperatures above and below these local transitions, the quantum yields fit eq 3 well. Only the K1W mutant exhibits no transition, resembling more closely the behavior of free, unblocked tryptophan, presumably due to the conformational lability and high level of solvent exposure of the N-terminal residue. (This mutant is discussed in more detail at the end of the Results.)

The behaviors of the quantum yields of the various tryptophan mutants differ strongly in two respects: first, in whether their quantum yield increases or decreases upon local unfolding; and second, in the slope of the asymptotic lines before and especially after the thermal transition. With regard to the first point, the change in the quantum yield upon local unfolding is determined by the relative change in the level of exposure to the solvent and in the removal of the tryptophan from the presence of quenching residues in the native structure, e.g., disulfide bonds. Thus, the quantum yields increase for the F8W, Y73W, Y92W, Y115W, and V124W mutants, all of which are close to local quenching groups, particularly the disulfide bonds between residues 40 and 95, 65 and 72, and 58 and 110. Hence, the tryptophans are no longer juxtaposed near these residues in the thermally unfolded state, indicating that the native structure is not exactly preserved. In contrast, the quantum yields decrease upon thermal denaturation for the mutants K1W, D38W, Y76W, and K104W, most likely corresponding to a simple increase in their levels of exposure to the solvent with the concomitant increase in the extents of solvent quenching.

However, it should be noted that the first group correlated with those mutants whose emission maxima shifted significantly upon thermal denaturation, indicating that thermal unfolding led to both higher levels of exposure of tryptophan residues to the solvent and spatial separation from adjacent quenching groups, as mentioned above. The second group correlated with those mutants whose emission maxima did not shift significantly upon thermal denaturation, indicating that, despite internal rearrangement of the tryptophan environment, the level of exposure to the solvent did not change, but quenching by adjacent groups and/or water molecules became more effective.

With regard to the second point, in every mutant except Y73W and Y115W, the slope $b$ of the asymptotic line (from Figure 6) after the thermal transition is greater than the slope before the transition, indicating increased thermal fluctuations of the tryptophan environment (greater freedom for the chromophore motions). Tyr-73 and Tyr-115 both occur in strongly hydrophobic segments of the native wild-type protein; thus, our data suggest that these segments do indeed form local hydrophobic clusters in which Trp-73 and Trp-115 occur in a more tightly packed environment (both being close to a disulfide bond) after thermal unfolding than before. This reduction in the slope $b$ is more pronounced for the Y115W mutant than for the Y73W mutant, consistent with the higher local hydrophobicity for Tyr-115 and the commensurately higher propensity of its local hydrophobic cluster (residues 106−118) to initiate conformational folding. These conclusions are consistent with the observed shifts in the emission maxima cited above for these mutants.

*Noncoincidence of Local and Global Unfolding.* With regard to the noncoincidence of the fluorescence unfolding curves and the main cooperative unfolding transition shown in Figure 6, it is important to realize that these low fluorescence transition temperatures are not the trivial result of a lower midpoint temperature in these mutants for the main cooperative unfolding transition. To illustrate this point, in Figure 7 we plot $f_u$, the fraction unfolded (as measured from the Trp fluorescence-detected transition curves of Figure 6), versus the temperature relative to the transition temperature for the main cooperative transition, as measured from the

far-UV CD spectra for the same mutants. The mutants fall into three basic groups. The first group consists of the mutants F8W, Y92W, K104W, and Y115W, whose fluorescence-detected transition temperatures are much lower (~10 °C lower) than their main cooperative transition temperature.

This discrepancy indicates that the corresponding regions of the polypeptide chain become destabilized well in advance of the main cooperative transition. The second group consists of the mutants D38W, Y73W, and Y76W, which unfold locally a few degrees (1.5−4.5 °C) in advance of the main cooperative transition. Finally, the mutant V124W forms a group by itself, in that local unfolding appeared at a temperature slightly higher than that of the global unfolding of the protein. This sequence of structural destabilization agrees with the Burgess−Scheraga structural model for thermal denaturation in RNase A (*15*), as discussed in the conclusions.

*Analysis of the K1W Mutant.* A more detailed analysis of the K1W mutant revealed a temperature dependence similar to that of free tryptophan in solution. This means that the N-terminal Trp residue did not interact with the rest of the protein to the same extent as did the tryptophan residues in other mutants. Both the free Trp and K1W data were modeled (Figure 8) by using the equation

$$\frac{1}{q} = 1 + \frac{k_0}{k_r} + A \exp(-E_A/RT) \qquad (4)$$

which has been shown to provide an accurate description of the temperature dependence of solvent-induced quenching of free Trp in solution (*46*, *65*, *71*). In this equation, $k_0$ represents the nonradiative temperature-independent intrinsic deactivation rate of the excited state, $k_r$ represents the inverse radiative fluorescence lifetime, $A$ is a constant, and $E_A$ is the activation energy of the quenching reaction. Both the free Trp and K1W data fit this equation well, whereas the K104W data (used here as a control) do not (Figure 8). The fitted activation energies for free Trp ($E_A = 40.2 \pm 0.08$ kJ/mol) and for the K1W mutant ($E_A = 58.6 \pm 0.8$ kJ/mol) disagree. This, as well as the difference in emission maxima, shows that the indole ring in the mutant K1W is attached to the surface of the protein without specific structurally dependent interactions.

## DISCUSSION

By using a multiple-spectroscopy approach, combined with site-directed insertion of fluorscent probes, this study provided evidence for multiple transitions in different parts of the RNase A molecule during thermal denaturation. With the exception of the V124W mutant, these local unfolding transitions occurred at temperatures lower than those of the global unfolding transition. The far-UV CD signal detected a cooperative loss of secondary structure (the global unfolding transition). The change in UV absorption, which depends on conformational changes in the vicinity of the tyrosine and tryptophan residues, detected changes in many sites over the entire tertiary structure. These sites were two clusters of tyrosine residues (25, 92, and 97 and 73, 76, and 115) as well as sites of tryptophan residues at different positions. The change in fluorescence properties of each single tryptophan residue reported specific local changes in conformation in the vicinity of the engineered indole side chains.

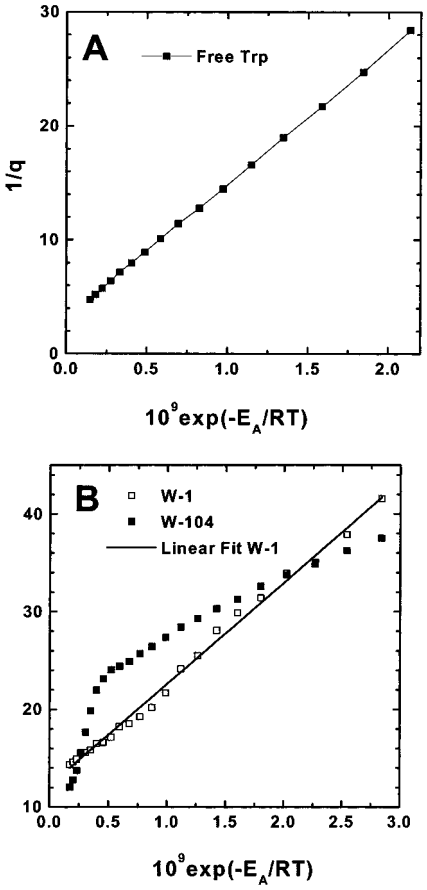


FIGURE 8: Temperature dependence of the reciprocal fluorescence quantum yield of the free tryptophan aqueous solution (A) and K1W and K104W mutants in 0.01 M sodium acetate buffer (pH 5.0) (B). The temperature axis is represented as $\exp(-E_A/RT)$. The straight lines show the best linear fit according to the highest correlation coefficient. The K1W mutant shows no fluorescence-detected transition.

*Far-UV CD Detected Thermal Denaturation.* The replacement of wild-type residues with tryptophan did not result in any detectable change in the calculated secondary structure content at room temperature. However, the far-UV CD spectra of the thermal transitions of the mutant proteins were not superimposable (see the Supporting Information). Specifically, the fine details of the denaturation transitions were affected by local interactions of the tryptophan side chains and loss of interactions of the replaced wild-type side chains, resulting in a lack of uniformity in the shape of the transition curves and in the midpoint temperatures. Notwithstanding the differences in the far-UV CD spectra, the perturbation caused by the site-specific replacement of the single wild-type residues with tryptophans was minimal since all the Trp mutants, with the exception of the two mutants near the active site (F8W and D38W), retained at least 85% of the wild-type RNase A enzymatic activity (Table 2).

*Effects of Inserted Tryptophans on Structure and Thermal Stability.* To use the site-specific insertion of tryptophans into RNase A to probe the characteristics of local and global thermal denaturation of the wild-type protein, it is essential to determine the extent to which the insertion of a nonnative tryptophan residue destabilizes the protein structure. Table 4 shows that a subgroup of mutations (K1W and Y92W) shifts the far-UV CD-detected transition midpoint temperature ($T_m$) to higher temperatures compared to that of wild-

type RNase A. The D38W and Y73W mutations slightly decrease the $T_m$ (<4 °C), and the Y76W, Y115W, and V124W mutations decrease the $T_m$ even more (4−6 °C) compared to that of the wild-type protein. Finally, the F8W and K104W mutations had the most destabilizing effect on the thermal stability of the proteins, decreasing the far-UV CD-detected $T_m$ by 9 and 11 °C, respectively. Overall, then, there is a minimal to moderate effect on protein stability from the substitution of a tryptophan residue at various locations within RNase A.

*Fluorescence versus UV Detection.* The number and characteristics of the transitions observed by the three spectroscopic techniques (UV, far-UV, CD, and fluorescence) differ significantly from each other. The transition temperatures of all the mutants as well as that of wt-RNase detected by UV absorption changes were between 4 and 9 °C lower than those of the corresponding far-UV CD-detected transitions. In addition, it is of interest to compare the transition temperatures measured for each mutant using tryptophan fluorescence to monitor local unfolding with those measured using far-UV CD and UV absorption to detect global transitions.

By comparison of the $T_m$ values determined by UV absorption and tryptophan fluorescence, two groups of RNase A Trp mutants can be distinguished. The group of the F8W, Y92W, K104W, and Y115W mutants had a higher $T_m$ detected by UV absorption, compared to the corresponding $T_m$ value determined by fluorescence. In contrast, the $T_m$ values determined by UV absorption were lower than the corresponding fluorescence-derived $T_m$ values for the D38W, Y73W, Y76W, and V124W mutants. This indicates that the local environment of the tryptophan residues in the mutants from the first group unfolded at temperatures lower than those of the cooperative change of the tertiary structure. For the second group, the situation is reversed.

*Fluorescence versus Far-UV CD Detection.* The comparison of local versus global unfolding is complicated by the unknown extent of structural perturbations attributed to the replacement of a wild-type RNase A residue with tryptophan. To estimate the extent of structural perturbation caused by the tryptophans, the far-UV CD-detected transition of each mutant protein was used as an internal reference. The denatured fraction, $f_u$, in Figure 7 shows the shift of the fluorescence-detected transitions of each RNase A Trp mutant protein relative to their corresponding far-UV CD-detected transition.

As can be seen in Figure 1, residue 104 connects the two $\beta$-sheet elements of the molecule and is part of the hydrophobic core with close contact to residues 79 on one side and 124 on the other. Thus, the change in the secondary structure occurs at temperatures higher than the change in the local environment of the tryptophan ring. Residue 8 is part of helix 1. Residues 92 and 115 are located between two strands in $\beta$-sheets 1 and 2, respectively, and can undergo local changes while the secondary structures are still stable. Tryptophans 38, 73, and 76 of the second group had the main transition close to that detected by far-UV CD.

From Figure 7, it seems that, of the first group, Trp-104 and Trp-115 showed a complete single fluorescence-detected transition which overlapped the pretransition detected by the far-UV CD signal. The local environments of residues 104 and 115 underwent a full transition associated with only small changes in the secondary structure of the molecule. Hence, for these mutants, it seems reasonable to conclude that the local changes are not coupled to the cooperative denaturation of the secondary structure of the whole molecule.

The V124W mutant was an exception showing the higher stability of the local structure than the secondary and tertiary structure. This is probably due to the replacement of Val-124 with the larger more hydrophobic Trp. The more hydrophobic indole of Trp-124 in the nonstructured C-terminal oligopeptide can be attached to adjacent $\beta$-strands and become almost free only after the disruption of the $\beta$-strands upon heating. Trp-73 is involved in a $\beta$-strand, and the coincidence of the far-UV CD- and fluorescence-detected transition (Figure 7) is not surprising.

The second group (Trp-38, -73, and -76) undergoes local changes in conformation only in the main cooperative transition, although residues 38 and 76 are not part of secondary structure elements. This is a manifestation of the interaction of these chain sections with the secondary structure backbone of the molecule.

The K1W mutant differed from the other mutants: the secondary and tertiary structures unfolded at higher temperatures than for wild-type protein, but local structure around Trp-1 did not show any transition. According to the fluorescence spectrum of K1W, centered at 343−344 nm at high and low temperatures, Trp-1 is a solvent-exposed residue with limited motion of the indole ring. This absence of a thermally induced conformational transition both in the quantum yield and in the spectra may be the result of surface binding of the solvent-exposed indole side chain to some part of the protein. Evidently, this attachment led to some stabilization of the protein molecule and a shift of the global thermal transition.

*Two-Step Transitions of Wild-Type and Mutant RNase A.* The thermal unfolding study of wild-type RNase A with calorimetric and optical detection indirectly suggested a two-step transition, the first of which is a pretransition with nonmeasurable heat absorption (*14*, *18*, *35*, *67*, *70*). In the study presented here, it is shown that the pretransition can be characterized by some changes in secondary and tertiary structures as measured by the three spectroscopic methods. This requires further investigation by recording full far-UV CD spectra of the whole molecule, which is beyond the scope of this investigation.

The two-step transition was found for all mutants even though the mutations caused shifts in the $T_m$'s. This shows that the two-step transition is a property of the whole molecule and not just a reflection of local unfolding events.

*Summary of the Features of the Thermal Unfolding.* The replacement of different residues in RNase A with tryptophan did not affect the protein structure at room temperature (as reflected by the far-UV CD spectra and the enzymatic activities) but influenced the thermal denaturation pathway. However, the reversibility of the thermal denaturation transition was not perturbed. The unfolding of the secondary structure and local tertiary structure at the positions studied was not complete at the end of the transition. For all the mutants, the transition temperatures derived from the UV absorbance (tertiary) were lower then those derived from the corresponding far-UV CD (secondary) measurements. This indicates that the unfolding of the tertiary structure preceded the unfolding of the secondary structure which is in line with the general notion of a hierarchy of protein denaturation.

The differences in the denaturation transition temperatures detected by tryptophan fluorescence and by far-UV CD are relatively small (0−11 °C), and the temperature ranges overlapped. This indicates that no molten-globule-like intermediate (*68*) could be stabilized as a dominant conformer. Mutations caused shifts of both types of transitions, which indicates that denaturation of secondary structures was evidently affected in part, or even initiated, by some changes in the tertiary structure.

Despite this close coupling of secondary and tertiary structure, the current measurements indicate that two, perhaps three, thermally induced transitions occur during the thermal unfolding of RNase A. The pretransition is associated with a few changes at the tertiary level of the structure. A possible scenario for the order of thermal denaturation of the RNase A molecule, based on our data, is as follows: First, nonlocal tertiary interactions around the C-terminal hydrophobic core are weakened. This includes changes in the local environment and contacts around residues 8, 104, and 115. In the crystal structure (*33*), these three residues are involved in nonlocal contacts between secondary structure elements that are stable at the pretransition temperatures. Residue 8 is in contact between helix I and the C-terminal loop; residue 104 is in contact with residue 124 and with $\beta$-sheet 2, and residue 115 is part of the contact between the C-terminal loop and the loop formed by the segment of residues 62−74. Residue 92 also shows a local change of microenvironment, perhaps due to loosening of the contact between the adjacent chain reversal loops (residues 36−39 and 91−94). Our data further suggest that the second local step in the thermal unfolding of RNase A may involve local conformational changes that are closely associated with the cooperative main transition of the secondary structure, including the microenvironment of residues 73, 76, and 38. From the crystal structure (*33*), it is known that residues 73 and 76 are part of the loop that forms a contact with the C-terminal loop, and residue 38 is part of the loop that forms a contact with the chain reversal segment of residues 91−94. The third phase of the thermal denaturation, which is in the last part of the cooperative secondary structure unfolding, likely involves loss of the loop structure between residues 104 and 124, detected by changes of the fluorescence of Trp-124. This can be due to the hydrophobic nature of the interactions between residues in the C-terminal loop (*67*), as was also found by Beals et al. (*69*), who showed that the loop structure of the 20 C-terminal-residue fragment (O-T-16) was stabilized by hydrophobic interactions.

These data provide clear evidence for significant structural changes prior to the main cooperative unfolding transition. Further, they support the Burgess−Scheraga model (*15*) [as modified by Matheson and Scheraga (*18*, *70*)] for the specific sequence of structures progressively destabilized during equilibrium thermal unfolding of RNase A. In agreement with that model, there appears to be a pretransition in the range of 30−45 °C (well below the main cooperative transition near 62 °C), in which the interaction of helix I (residues 3−13) with the major hydrophobic core is loosened, providing increased conformational freedom to the side chains involved in the interface (which includes residue 8 on one side and residues 104 and 115 on the other) while preserving the overall backbone topology.

Moreover, the relative transition midpoint temperatures of the mutants measured by far-UV CD and by Trp fluorescence are in general agreement with the sequence of structures hypothesized by the Burgess−Scheraga model to be destabilized by thermal unfolding. The side chain of Trp-92 is the first structure to be changed early in the unfolding. The same is true for the relaxation of the tertiary interactions of the C-terminal $\beta$-hairpin and the N-terminal helix, judging from the relative transition midpoint temperatures of Trp-8, Trp-104, and Trp-115. The structures changed at higher temperatures are the major $\beta$-hairpin (residues 79−102) and the loop (residues 65−72), as seen by the relative transition midpoint temperatures of Trp-38 and Trp-76. One discrepancy, however, with the Burgess−Scheraga model is the remarkable stability observed here for the C-terminal residue Val-124, which was observed to be cleaved by carboxypeptidase slightly before the main cooperative transition (*26*). Val-124 forms a strong backbone hydrogen bond with His-105 in the native structure, which has been conjectured to contribute to the strong pH sensitivity of the folding stability of RNase A (*15*). This discrepancy may possibly be due to the effect of the tryptophan mutation since Val-124 participates in the hydrophobic core, and the tryptophan side chain is much larger than that of valine.

Unfortunately, our experiments cannot test other aspects of the Burgess−Scheraga model, e.g., whether helix II (residues 25−35) becomes destabilized in the temperature range of 30−45 °C, in concert with the changes occurring in the interface between helix I (residues 3−13) and the major hydrophobic core. This is structurally plausible, since helix II interacts with helix I through a very strong side chain−side chain hydrogen bond between Asp-14 and Tyr-25 (*59*); thus, the structural destablization of helix I and helix II should be coupled. Raman spectroscopy data indicate that this strong hydrogen bond is maintained up to the main cooperative transition (*27*, *31*).

## ACKNOWLEDGMENT

We thank M. A. McDonald for help in cloning and expression of wild-type and mutant RNase, Dr. S. Yu. Venyaminov (Mayo Foundation, Rochester, MN), Dr. N. J. Greenfield (University of Medicine and Dentistry of New Jersey-Robert Wood Johnson Medical School, Newark, NJ) for programs and consulting to calculate the secondary structure from the far-UV CD spectra, and Dr. W. J. Wedemeyer for helpful comments on the manuscript.

## SUPPORTING INFORMATION AVAILABLE

CD and UV transition curves of all nine mutants. This material is available free of charge via the Internet at http://pubs.acs.org.

## REFERENCES

1. Harrington, W. F., and Schellman, J. A. (1956) *C. R. Lab. Carlsberg, Ser. Chim. 30*, 21−43.
2. Hermans, J., Jr., and Scheraga, H. A. (1961) *J. Am. Chem. Soc. 83*, 3283−3292.
3. Privalov, P. L., and Khechinashvili, N. N. (1974) *J. Mol. Biol. 86*, 665−684.
4. Seshadri, S., Oberg, K. A., and Fink, A. L. (1994) *Biochemistry 33*, 1351−1355.

5. Eberhardt, E. S., Wittmayer, P. K., Templer, B. M., and Raines, R. T. (1996) *Protein Sci. 5*, 1697−1703.
6. Dodge, R. W., and Scheraga, H. A. (1996) *Biochemistry 35*, 1548−1559.
7. Liu, Y., and Sturtevant, J. M. (1996) *Biochemistry 35*, 3059−3062.
8. Arnold, U., and Ulbricht-Hofmann, R. (1997) *Biochemistry 36*, 2166−2172.
9. Tanimizu, N., Ueno, H., and Hayashi, R. (1998) *J. Biochem. 124*, 410−416.
10. Denisov, V. P., and Halle, B. (1998) *Biochemistry 37*, 9595−9604.
11. Qi, P. X., Sosnick, T. R., and Englander, S. W. (1998) *Nat. Struct. Biol. 5*, 882−884.
12. Pace, C. N., Grimsley, G. R., Thomas, S. T., and Makhatadze, G. I. (1999) *Protein Sci. 8*, 1500−1504.
13. Scott, R. A., and Scheraga, H. A. (1963) *J. Am. Chem. Soc. 85*, 3866−3873.
14. Privalov, P. L., Tiktopulo, E. I., and Khechinashvili, N. N. (1973) *Int. J. Pept. Protein Res. 5*, 229−237.
15. Burgess, A. W., and Scheraga, H. A. (1975) *J. Theor. Biol. 53*, 403−420.
16. Benz, F. W., and Roberts, G. C. K. (1975) *J. Mol. Biol. 91*, 345−365.
17. Mathews, C. R., and Westmoreland, D. G. (1975) *Biochemistry 14*, 4532−4538.
18. Matheson, R. R., Jr., and Scheraga, H. A. (1979) *Biochemistry 18*, 2437−2445.
19. Mathews, C. R., and Froebe, C. L. (1981) *Macromolecules 14*, 452−453.
20. Labhardt, A. M. (1982) *J. Mol. Biol. 157*, 331−355.
21. Swadesh, J. K., Montelione, G. T., Thannhauser, T. W., and Scheraga, H. A. (1984) *Proc. Natl. Acad. Sci. U.S.A. 81*, 4606−4610.
22. Talluri, S., and Scheraga, H. A. (1990) *Biochem. Biophys. Res. Commun. 172*, 800−803.
23. Zhang, J., Peng, X., Jonas, A., and Jonas, J. (1995) *Biochemistry 34*, 8631−8641.
24. Torrent, J., Connelly, J. P., Coll, M. G., Ribó, M., Lange, R., and Vilanova, M. (1999) *Biochemistry 38*, 15952−15961.
25. Laity, J. H., Montelione, G. T., and Scheraga, H. A. (1999) *Biochemistry 38*, 16432−16442.
26. Burgess, A. W., Weinstein, L. I., Gabel, D., and Scheraga, H. A. (1975) *Biochemistry 14*, 197−200.
27. Chen, M. C., and Lord, R. C. (1976) *Biochemistry 15*, 1889−1897.
28. Matheson, R. R., Jr., Dugas, H., and Scheraga, H. A. (1977) *Biochem. Biophys. Res. Commun. 74*, 869−876.
29. Howarth, O. W. (1979) *Biochim. Biophys. Acta 576*, 163−175.
30. Chavez, L. G., Jr., and Scheraga, H. A. (1980) *Biochemistry 19*, 996−1004.
31. Gilbert, W. A., Lord, R. C., Petsko, G. A., and Thamann, T. J. (1982) *J. Raman Spectrosc. 12*, 173−179.
32. Sendak, R. A., Rothwarf, D. M., Wedemeyer, W. J., Houry, W. A., and Scheraga, H. A. (1996) *Biochemistry 35*, 12978−12992.
33. Wlodawer, A., Svensson, L. A., Sjölin, L., and Gilliland, G. L. (1988) *Biochemistry 27*, 2705−2717.
34. del Cardayré, S. B., Ribó, M., Yokel, E. M., Quirk, D. J., Rutter, W. J., and Raines, R. T. (1995) *Protein Eng. 8*, 261−273.
35. Laity, J. H., Lester, C. C., Shimotakahara, S., Zimmerman, D. E., Montelione, G. T., and Scheraga, H. A. (1997) *Biochemistry 36*, 12683−12699.
36. Woody, R. W. (1995) *Methods Enzymol. 246*, 34−71.
37. Venyaminov, S. Yu., and Yang, J. T. (1996) in *Circular Dichroism and the Conformational Analysis of Biomolecules* (Fasman, G. D., Ed.) pp 69−107, Plenum Press, New York.
38. Provencher, S. W., and Glöckner, J. (1981) *Biochemistry 20*, 33−37.
39. Provencher, S. W. (1982) *Comput. Phys. Commun. 27*, 213−227.
40. Provencher, S. W. (1982) *Comput. Phys. Commun. 27*, 229−242.
41. Sreerama, N., and Woody, R. W. (1993) *Anal. Biochem. 209*, 32−44.
42. Venyaminov, S. Yu., Baikalov, I. A., Shen, Z. M., Wu, C.-S. C., and Yang, J. T. (1993) *Anal. Biochem. 214*, 17−24.
43. Leach, S. J., and Scheraga, H. A. (1960) *J. Am. Chem. Soc. 82*, 4790−4792.
44. Sela, M., and Anfinsen, C. B. (1957) *Biochim. Biophys. Acta 24*, 229−235.
45. Harris, D. A. (1987) in *Spectrophotometry and Spectrofluorimetry: a practical approach* (Bashford, C. L. and Harris, D. A., Eds.) p 49, IRL Press, Oxford, U.K.
46. Weinryb, I., and Steiner, R. F. (1971) in *Excited States of Proteins and Nucleic Acids* (Steiner, R. F., and Weinryb, I., Eds.) pp 277−318, Plenum Press, New York.
47. Permyakov, E. A. (1993) *Luminescent spectroscopy of proteins*, CRC Press, Boca Raton, FL.
48. Gottfried, D. S., and Haas, E. (1992) *Biochemistry 31*, 12353−12362.
49. Thannhauser, T. W., and Scheraga, H. A. (1985) *Biochemistry 24*, 7681−7688.
50. Weast, R. C., Ed. (1976) *Handbook of Chemistry and Physics*, 57th ed., p F-51, CRC Press, Cleveland.
51. Pflumm, M. N., and Beychok, S. (1969) *J. Biol. Chem. 244*, 3973−3981.
52. Pflumm, M. N., and Beychok, S. (1969) *J. Biol. Chem. 244*, 3982−3989.
53. Takahashi, S., Kotani, T., Yoneda, M., and Ooi, T. (1977) *J. Biochem. 82*, 1127−1133.
54. Simpson, R. T., and Vallee, B. L. (1966) *Biochemistry 5*, 2531−2538.
55. Simmons, N. S., and Glazer, A. N. (1967) *J. Am. Chem. Soc. 89*, 5040−5042.
56. Strickland, E. H. (1974) *CRC Crit. Rev. Biochem. 2*, 113−175.
57. Navon, A., Ittah, V., Landsman, P., Scheraga, H. A., and Haas, E. (2001) *Biochemistry 40*, 105−118.
58. Strickland, E. H. (1972) *Biochemistry 11*, 3465−3474.
59. Scheraga, H. A. (1967) *Fed. Proc. 26*, 1380−1387.
60. Sosnick, T. R., and Trewhella, J. (1992) *Biochemistry 31*, 8329−8335.
61. Arnold, U., Rucknagel, K. P., Scvhierhorn, A., and Ulbricht-Hofmann, R. (1996) *Eur. J. Biochem. 237*, 862−869.
62. Szabo, A. G., and Rayner, D. M. (1980) *J. Am. Chem. Soc. 102*, 554−563.
63. Bushueva, T. L., Busel, E. P., and Burstein, E. A. (1978) *Biochim. Biophys. Acta 534*, 141−152.
64. Permyakov, E. A., and Burstein, E. A. (1984) *Biophys. Chem. 19*, 265−271.
65. Turoverov, K. K. (1969) *Opt. Spektrosk. 26*, 564−570.
66. Allen, D. L., and Pielak, G. J. (1998) *Protein Sci. 7*, 1262−1263.
67. Matheson, R. R., Jr., and Scheraga, H. A. (1978) *Macromolecules 11*, 819−829.
68. Ptitsyn, O. B. (1995) *Trends Biochem. Sci. 20*, 376−379.
69. Beals, J. M., Haas, E., Krausz, S., and Scheraga, H. A. (1991) *Biochemistry 30*, 7680−7692.
70. Matheson, R. R., Jr., and Scheraga, H. A. (1979) *Biochemistry 18*, 2446−2450.
71. Longworth, J. W. (1971) in *Excited States of Proteins and Nucleic Acids* (Steiner, R. F., and Weinryb, I., Eds.) pp 319−484, Plenum Press, New York.


BI001945W